Passivation Agents and Conditions for Mo_2C and W_2C: Effect on Catalytic Activity for Toluene Hydrogenation

*Ali Mehdad, Rolf E. Jentoft, and Friederike C. Jentoft**

School of Chemical, Biological & Materials Engineering
University of Oklahoma, Norman, OK 73019, USA

* Author to whom correspondence should be addressed:
F.C. Jentoft, present address: Department of Chemical Engineering, University of Massachusetts, 159 Goessmann Laboratory, 686 North Pleasant Street, Amherst, MA 01003-9303, Email fcjentoft@umass.edu

Abstract

The passivation and reactivation of Mo_2C and W_2C was investigated by thermogravimetry with effluent gas analysis, and by comparison of the toluene hydrogenation activity of fresh carbides with that of passivated and reactivated carbides (20 bar, H_2 : toluene = 33, 150 or 200 °C, WHSV = 10 or 20 g g_{cat}^{-1} min^{-1}). Contrary to the literature, CO_2 and H_2O were unsuitable passivation agents for Mo_2C. Mo_2C and W_2C reacted readily with O_2 at 40 °C. The mass gained during oxidation could be quantitatively removed through reduction in 1 bar H_2 at 300 °C (Mo_2C) or 400 °C (W_2C). The rate of toluene conversion was fully recovered only for Mo_2C that had been passivated with an initial O_2 concentration of 0.1 vol.% and not for other passivation conditions or for W_2C. Intervening operation of toluene hydrogenation at 300 or 400 °C enhanced the activity of samples that were previously oxidized and reduced or harshly reduced. This enhancement suggests that carbide formation is possible at milder temperatures than typically employed.

Keywords: molybdenum carbide, tungsten carbide, structure sensitivity, aromatic ring hydrogenation, methylcyclohexane, temperature-programmed reduction, X-ray diffraction, thermal analysis.

1. Introduction

Since Levy and Boudart reported that tungsten carbide shows Pt-like behavior in that it can 1) catalyze the oxidation of H_2 at room temperature, 2) catalyze the reduction of WO_3 by moist H_2 to form H_xWO_3 at room temperature, and 3) catalyze the isomerization of 2,2 dimethylpropane to 2-methylbutane, early transitional metal carbides have gained interest as potentially less costly and sustainable substitutes for precious metal catalysts [1]. Moreover, transition metal carbides are refractory materials that will not easily sinter, and have been reported to be resistant to sulfur poisoning [2,3]. These qualities make metal carbides promising materials for application as catalysts for a wide variety of reactions. Metal carbides have been tested for hydrogenation [3], hydrotreating [4], methane dehydroaromatization [5], partial oxidation of methane to syngas [6], ammonia decomposition [7], water gas shift [8], and, more recently, hydrodeoxygenation [9].

Transition metal carbides with high surface area, as is desirable for catalysis, are usually prepared by heating an oxidic precursor containing the metal in a reducing atmosphere that contains carbon [10,11]. The transition metal in the precursor material is at an oxidation state greater than zero, and the carburization process starts with reduction, followed by the intercalation of carbon, usually at temperatures between 600 and 900 °C. In the case of molybdenum and tungsten, the carbide phases initially obtained by this process are hexagonal Mo_2C [10] and hexagonal W_2C, whereas at higher temperatures hexagonal WC forms [6].

The fresh surfaces of carbides are reactive towards O_2 and can be pyrophoric. Ideally, pyrophoric materials would be investigated without contact with air [12]. However, it is common practice, as reported in the literature [10,11,13], to passivate the surfaces of transition metal carbides to transfer the materials from the synthesis reactor to characterization equipment or a catalytic test reactor. The ability to passivate and re-reduce a surface is also pertinent for transport and storage in conjunction with commercial use. The majority of the literature on carbide catalysts reports results obtained with carbides that are passivated by flowing low concentrations of O_2 in an inert diluent over the fresh carbide, and it is common practice to use 0.5 or 1% O_2 [10,11,13-16]. However, control of the degree of oxidation can be an issue. For example, Leclercq et al. tested the stability of WC and W_2C during heating in 2 vol.% O_2 [17]. Bulk oxidation of carbon-coated WC commenced at 400 °C, and continued to WO_3 without detection of intermediate oxides by X-ray diffraction (XRD). Consequently, other passivation techniques have been explored.

Zhao et al. found that an amorphous carbon layer on the surface of FeC particles enhanced resistance to oxidation [18]. McBreen and co-workers reported the anchoring of alkylidene layers on molybdenum carbide by reacting the carbide with cyclobutanone at sub-ambient temperatures [19,20]. The alkylidene groups are attached to the molybdenum atoms. The surface was inferred to be inert because of additional carbon deposited during alkylidene layer formation, and perhaps because of oxygen from the ketone that also bonds with the molybdenum. Warren et al. investigated the use of water as a passivation agent [21]. They monitored the oxidation of tungsten carbide surfaces and found that a 6 Å layer of oxide formed when the tungsten carbide surface was exposed to air at a temperature of 25 °C, but that "when WC was exposed to water, it resisted further oxidation". Wu et al. [22] investigated the use of O_2, water, and carbon dioxide for the passivation of molybdenum carbide supported on aluminum oxide, and reported that the carbide surface that was passivated in either CO_2 or water could be more fully regenerated than that passivated in O_2. The conclusions were based on IR spectra of adsorbed carbon monoxide, which was used as a probe molecule to identify changes to the molybdenum oxidation state and the number of surface sites that could be regenerated after passivation. Bogatin et al., who investigated the magnetic properties of neodymium-iron-boron nitrides and carbides, reported passivating their powdered carbides with CO_2 or N_2 at temperatures between 125 and 300 °C [23]. The passivation resulted in surface neodymium carbides and nitrides that stabilized the material although neodymium oxides were observed after storage.

It is important to remember that there are two measures of the success of a passivation treatment for catalysts: 1) protection of the sample from air, and 2) successful desorption/re-reduction and regeneration of the active carbide surface. Only few investigations address the regeneration of passivated carbides. Shou et al. heated a passivated molybdenum carbide in a 1:1 mixture of CO and H_2 to 300 °C and found that, relative to a non-passivated sample, the activity for Fischer–Tropsch synthesis was 37% lower, and alcohol production was reduced by an order of magnitude [24]. Leary et al. investigated an O_2-passivated Mo_2C surface and concluded that at a temperature of 130 °C, the oxygen is mobile in the bulk carbide, and that during temperature-programmed reduction (TPR), first surface reduction occurs at 206 °C, and then oxygen diffuses out of the carbide bulk at 300 °C [25]. Leclercq et al. sought to remove carbon from the surfaces of WC, W_2C, Mo_2C and Cr_3C_2 through treatment with H_2 [17]. The authors found that removal of excess carbon from WC and Mo_2C could be accomplished with H_2 at 700 °C, resulting in clean

and stable carbides, whereas W_2C was only stable up to 400 °C, and at higher temperature continued to lose carbon and transformed into metallic tungsten. These results indicate that re-activation may be imperfect, and the carbide may even be destroyed during re-reduction in H_2.

Understanding the interaction of oxygen with the surface of metal carbides is not only important for passivation after preparation, but may also be of interest for catalytic reactions with oxygen-containing molecules such as Fischer–Tropsch synthesis, water gas shift, or biomass upgrading [26]. The presence of oxygen on the surface of metal carbides can change product selectivity [27,28], which in some cases was explained with the formation of acid sites [29,30].

The goal of this work was to better understand the effect of compounds that have been reported as passivation agents for transition metal carbides, specifically O_2, CO_2 and H_2O. Mo_2C and W_2C were chosen because they are both catalytically active for a wide variety of reactions and because the metal oxides have distinctly different stabilities. Thermogravimetry was used to monitor weight gain and the effectiveness of the passivation. The metal carbides were regenerated under various gas atmospheres and pressures, and the effect of surface passivation and re-activation on catalytic activity was investigated using an in-situ synthesized carbide as a benchmark. Toluene served as a test reactant; ring hydrogenation probes metallic sites while subsequent ring contraction can indicate acid sites and residual oxygen.

2. Experimental Section

2.1. Thermogravimetric analysis of carbide synthesis, passivation, and re-activation

2.1.1. Introduction

Fresh Mo_2C and W_2C were prepared by temperature-programmed (TP) reaction of MoO_3 or WO_3 in a thermogravimetric analyzer (TGA), as described in Sections 2.1.2 and 2.1.3. Passivation, test of the passivation, and temperature-programmed reduction at atmospheric pressure (Sections 2.1.4 through 2.1.7) were conducted subsequently in the same apparatus without exposing the sample to the ambient. Each passivation treatment was applied to a freshly prepared carbide.

2.1.2. TGA Apparatus and materials

A Netzsch STA 449 F1 thermogravimetric analyzer (TGA) with differential scanning calorimeter (DSC) was connected to a mass spectrometer (QMS 403 C Aëolos) via a stainless-steel capillary. TP reaction runs with empty crucibles were used to correct for sample holder

buoyancy and gas viscosity artifacts. MS signals were generally normalized to initial sample mass. Ethane (99.95%, Matheson), was used as received; other gases were further purified prior to use. Air (zero grade, Airgas) and H_2 (ultra-high purity, Airgas) were passed through a moisture trap (Agilent, MT400-2), CO_2 (instrument grade, Airgas) was passed through an oxygen trap (Z-Pure Glass Indicating Oxygen Trap), and argon (ultra-high purity, Airgas) was passed through dual moisture and oxygen trap (Z-Pure Dual Purifier).

2.1.3. Carbide synthesis protocol

Synthesis methods were similar to those reported in the literature [6,11]. The syntheses were carried out at atmospheric pressure. The gas mixture for carburization was 5 ml/min ethane, 35 ml/min H_2, and 10 ml/min argon; all flow rates at STP. Either MoO_3 (99.95%, Alfa Aesar) or WO_3 (99.995%, Aldrich) were heated in the carburization gas mixture from room temperature to 450 °C with a temperature ramp of 5 °C/min, and from 450 °C to the final temperature, with a temperature ramp of 2 °C/min. The final synthesis temperatures for Mo_2C and W_2C were 650 °C and 700 °C, respectively. The samples were held at the final temperature for 1.5 h.

2.1.4. Passivation with O_2

Passivation of freshly prepared carbide catalysts with O_2 was carried out isothermally at 40 °C using air diluted in argon with total flow rates between 50 and 400 ml/min. Criteria for the temperature were (i) ability to control the temperature inside the thermobalance by being slightly above laboratory temperature, and (ii) prevention of bulk oxidation while completing the passivation within reasonable time. The "1% O_2" passivation was 16 h of 1% O_2 (by volume) followed by 16% O_2 for 1 h to test the effectiveness of the passivation. The "0.1% O_2" passivation started with 0.1% O_2 for 3 h, followed by 0.5% O_2 for 3 h, 1.0% O_2 for 3 h and finally 16% O_2 for 3 h.

2.1.5. Passivation with CO_2

In order to test passivation of freshly prepared Mo_2C in CO_2, the carbide was heated to 100 °C in flowing argon and then the gas phase was switched to 30% CO_2 in argon for 3 h. The sample was then cooled to 40 °C in argon and, subsequently, the gas was switched to 16% O_2/Ar to determine if the sample had been passivated. The behavior of molybdenum carbide was also tested using temperature-programmed reaction in 30% CO_2. The sample, initially at 35 °C, was purged

for 20 min in 100% Ar followed by 20 min in 30% CO_2/Ar with a total flow rate of 100 ml/min. The temperature was increased from 35 to 800 °C with a ramp of 5 °C/min in 30% CO_2/Ar.

2.1.6. Passivation with H_2O

Argon (120 ml/min) was bubbled through deionized water in a saturator that was submerged in a 20 °C water bath. The resulting water partial pressure was 2.3 kPa. The water-saturated argon was then mixed with 30 ml/min dry argon in the TGA. Passivation in the presence of water was initially tested at 110 °C. The freshly carburized Mo_2C sample was first heated in argon to 110 °C and held at 110 °C for 1 h. The gas flow was then switched to 150 ml/min of 1.8% water in argon for 2 h (still at 110 °C); the gas flow was then switched back to pure argon followed by cooling to 40 °C. The sample was subsequently exposed to 16% O_2/Ar to test for passivation. TP reaction in a water-containing atmosphere started with a 1 h purge in Ar at 110 °C. The gas phase was then switched to 1.8% water in argon and the sample was heated to 800 °C at 5 °C/min.

2.1.7. Temperature-programmed reduction (TPR)

The TPR experiments were carried out in the TGA on about 12 mg of sample. The total flow rate was 50 ml/min of 80% H_2 in argon. The temperature was increased from 40 to 700 °C with a ramp of 5 °C/min and then held for 1 h.

2.2. Catalytic toluene hydrogenation with in situ or ex situ synthesized carbides

2.2.1. Reactor

The flow reactor was a 0.18 inch inner diameter stainless steel tube with Swagelok® connections equipped with an Eldex liquid feed pump. The reactor was loaded with carbide powder or an appropriate amount of oxide powder (in-situ sample preparation) to have a final amount of 50 mg of Mo_2C or 100 mg of W_2C. The length of the bed was increased by adding 200 to 300 mg SiC (Aldrich, 200-450 mesh) to avoid channeling and local heating. The reactor was placed into a 2 ft long electrical furnace, and the temperature was controlled using a thermocouple inside the reactor at the bottom of the catalyst bed.

2.2.2. In situ synthesis of carbides

Fresh carbides for catalytic testing were synthesized in situ in the stainless steel reactor. The gas flow was 10% ethane in H_2 with a total flow rate of 50 ml/min at near atmospheric pressure

with the same temperature program as described for sample preparation using the TGA (Section 2.1.2). To measure the surface area of fresh carbides, the reactor was isolated and transferred to a glove box. Inside the glove box, the samples were transferred to a N_2 physisorption tube with a seal frit (Micromeritics) and then removed from the glove box for analysis.

2.2.3. Reactivation of passivated carbides

Before the catalytic test, passivated Mo_2C was regenerated by reduction in flowing H_2 at 300 °C and 1 or 20 bar, for 2 h. Passivated W_2C was regenerated by reduction in H_2 at 400 °C and 1 bar or 20 bar, for 2 h. The gas flow was 150 ml/min, and the temperature ramp was 10 °C/min. A sample of 1% O_2-passivated Mo_2C was reactivated in the carburization mixture, 10% ethane in H_2 at a flow rate of 50 ml/min. A Pfeiffer Omnistar MS GSD 320 was optionally connected to the effluent line for gas phase analysis.

2.2.4. Vapor phase toluene hydrogenation

The catalytic reaction was carried out with gaseous reactants fed at 0.02 ml/min of liquid toluene (99.5%, Mallinckrodt Chemicals) and 150 ml/min STP H_2 (Ultra high purity, Airgas). The reactor total absolute pressure was 21 bar, which was controlled by a back pressure valve. Samples were tested sequentially at different temperatures, 150 °C for 4 h, 200 °C for 2 h, 300 °C for 2 h and cooled to 150 °C for 3 h for Mo_2C and 200 °C for 3 h, 300 °C for 2 h, 400 °C for 2 h and cooled to 200 °C for 2 h for W_2C. Products were analyzed every 30 min using an online HP 5890 GC with flame ionization detector (FID), equipped with a 30 m, 0.32 μm GASPRO column. Transfer lines to the GC were heated to ensure that no condensation occurred. The GC temperature program was, 5 min isothermal at 60 °C, then 10 °C/min to a final temperature of 240 °C, which was held for 4 min. Conversion of toluene is defined as the moles of toluene in the feed minus moles of toluene in the product divided by moles of toluene in the feed.

2.3. Characterization of carbide bulk structure and texture and CO chemisorption

Samples were characterized by X-ray diffraction (XRD) using a Bruker D8 instrument and Cu Kα radiation. The samples were measured in reflection geometry. The diffractograms were fit using the program Powdercell. The crystalline domain sizes were estimated from the full width at half maximum of the (101) reflections using the Scherrer formula and assuming no strain component and an instrument breadth of 0.23°. The resulting domain sizes can be considered an upper limit.

Surface areas were determined by the BET method using a Micromeritics ASAP 2010 and N_2 at -196 °C. Pore size distributions were determined from N_2 desorption isotherms by applying the BJH method. Unpassivated samples were transferred to the N_2 physisorption tube with seal frit in a glove box without coming in contact with air. Before measuring the surface area, the samples were degassed by evacuation at a temperature of 350 °C for 4 h.

CO pulse chemisorption was conducted using an AMI-200ip (Altamira Instruments), a gas composition of 20% CO/He, and a loop size corresponding to 58 μmol. Research grade (99.999%) CO was obtained from Matheson Gas. Prior to CO chemisorption, samples were reduced for 2 h in flowing H_2 at 300 °C (Mo_2C) or 400 °C (W_2C). After reduction, the gas flow was switched to helium, and the temperature was held for 1 h. Then, samples were cooled to 35 °C for CO pulse chemisorption. To analyze unpassivated samples, carburization was performed in the same tube as that used for chemisorption, and the tube was transferred to the chemisorption apparatus without contact of the carbide with air.

3. Results

3.1. Characterization of sample structure and surface area

The sample stoichiometry was determined by weight change during synthesis in the TGA. For both MoO_3 and WO_3 the weight loss during carbide synthesis occurred in two steps. During the first step in weight loss, the gas phase analysis showed only water, indicating reduction by hydrogen. During the second step in weight loss, the gas phase products were both water and CO_2, or a mixture of CO and CO_2, indicating that ethane also served as reductant. The first weight loss steps ended at about -11.2% and -7.0% weight change (inflection point) for MoO_3 and WO_3, respectively. The total weight loss until formation of the product carbides was -28.5% and -17.8% for MoO_3 and WO_3, respectively. The diffractograms of both carbides are presented in Figure 1. Comparison with powder diffraction files from the International Centre for Diffraction Data (ICDD) resulted in matches with # 00-035-0787, full IUPAC notation Mo_2C(*hP*3, $P6_3/mmc$) (NiAs type) and # 00-035-0776, IUPAC notation W_2C(*hP*3, $P\bar{3}m1$) (CdI_2 type). The diffractograms show relatively broad peaks consistent with very small crystalline domains, or with a disordered structure. The crystalline domain sizes were calculated to 6.6 nm and 7.3 nm for Mo_2C and W_2C, respectively.

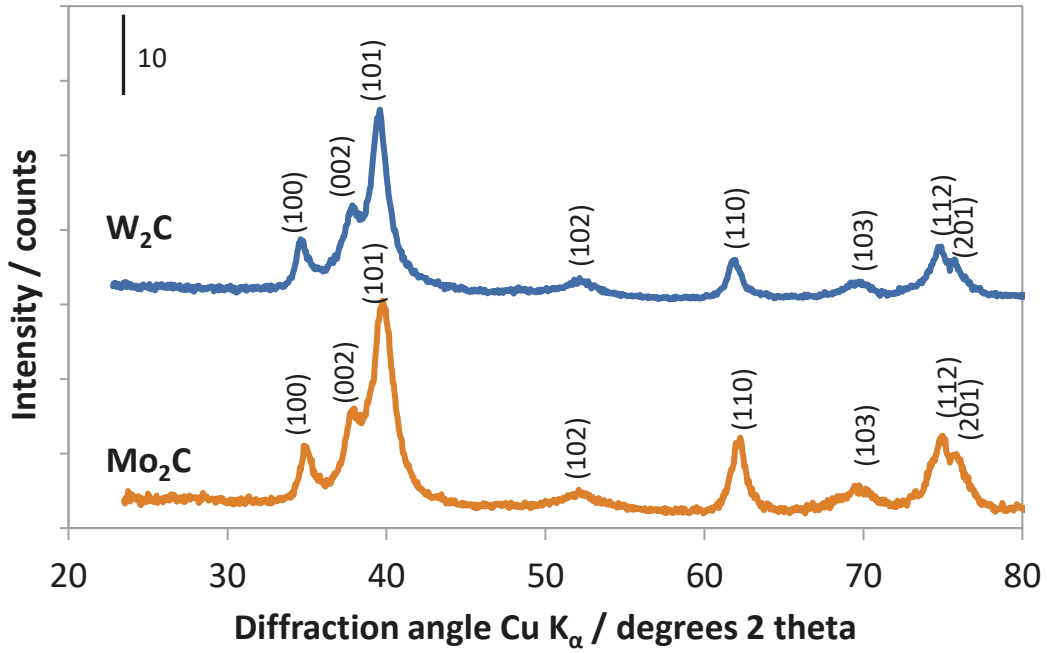

Figure 1: XRD of W_2C (top) and Mo_2C (bottom). Indexed with ICDD powder diffraction file # 00-035-0787 for Mo_2C and # 00-035-0776 for W_2C.

Surface areas of the carbides and the 1% O_2 passivated carbides are reported in Table 1. The fresh Mo_2C and W_2C samples had surface areas of 58 and 35 m^2/g, respectively. Both samples lost surface area during passivation in 1% O_2. The surface area of the Mo_2C sample was reduced to 43 m^2/g and the surface area of the W_2C sample was reduced to 23 m^2/g. For both samples, the pore volume decreased during passivation and the average pore diameter increased.

Table 1: N_2 physisorption data for Mo_2C and W_2C

Samples	***Surface area (m^2/g)***	***BJH average pore diameter (Å)[b]***	***BJH pore volume (cm^3/g)[b]***
Mo_2C Fresh	58	29	0.047
Mo_2C Passivated[a]	43	36	0.038
W_2C Fresh	35	73	0.072
W_2C Passivated[a]	23	98	0.044

[a] Passivated in 1% O_2

[b] Calculated from desorption branch of the isotherm.

3.2. Passivation with O_2, CO_2 and H_2O

Figure 2a shows the weight gain during passivation of Mo_2C at 40 °C in 1% O_2 and in slowly increasing O_2 concentration starting at 0.1% O_2. For the case of 1% O_2, the weight initially increases at a rate of 0.58%/min and then more slowly, leading to a 2% weight gain within 10 min. For the case of 0.1% O_2, the weight gain is initially 0.08%/min and the sample gains only 0.8% within the first 10 min. The higher oxygen concentration leads to a sharp and intense heat signal, whereas the lower concentration leads to a subdued heat effect (Figure 2b). Samples passivated at these low O_2 concentrations were then exposed to 16% O_2 to test stability at near-ambient conditions. Table 2 shows that the final weight gain (after exposure to 16% O_2) was 3.6% for the 1.0% O_2 passivated sample vs. 3.1% weight gain for the 0.1% O_2 passivated sample. Even after exposure to 16% O_2 for one or more hours, the samples continued to gain weight at a very slow rate. During passivation with O_2, the gas phase was monitored with a mass spectrometer. There were no detectable gas phase products.

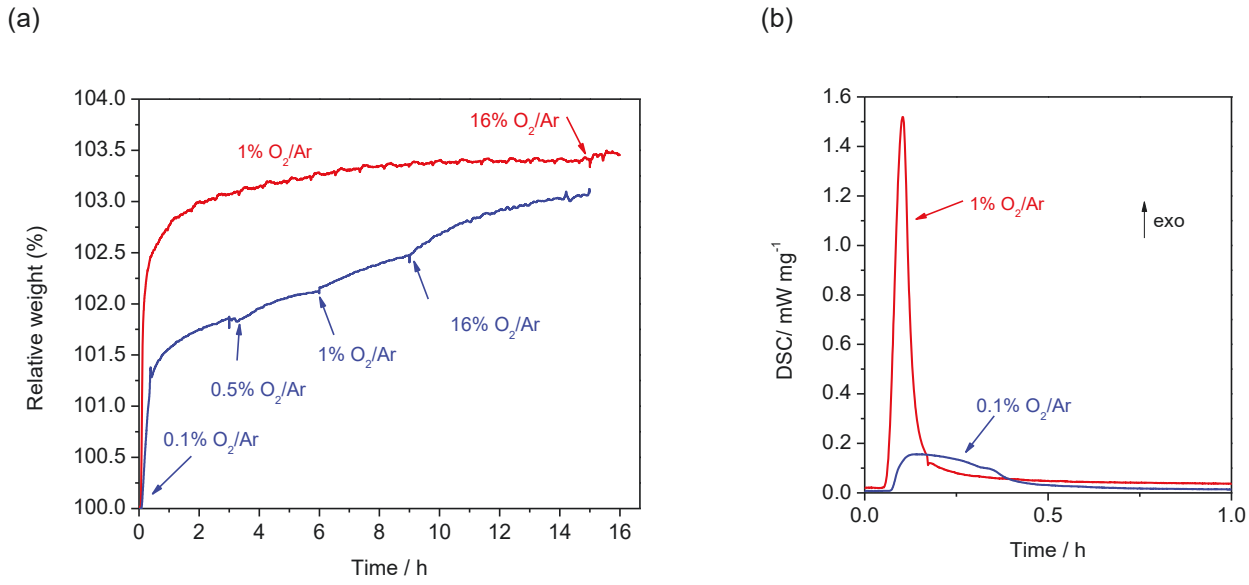

Figure 2: TGA of passivation of Mo_2C at a temperature of 40 °C in different concentrations of O_2: (a) weight increase, (b) heat signal.

Results for the passivation of W_2C in O_2 are presented in Table 2. The fresh tungsten carbide sample gained 2.5% of its initial weight when passivated in 0.1% O_2, and gained 2.8% of its initial weight when passivated in 1% O_2.

Table 2: Weight gained during passivation and lost during reactivation

Sample	*Weight change (%)*			*Oxygen/metal (molar ratio)*	
	Passivation[a]	*Reactivation*[a]	*Reactivation after storage*[b]	*Total*	*Surface*[c]
Mo_2C 1% O_2	+3.6	-3.5	-9.7	0.23	1.7
Mo_2C 0.1% O_2	+3.1	-2.9	-	0.20	1.5
W_2C 1% O_2	+2.8	-2.7	-	0.33	2.2
W_2C 0.1% O_2	+2.5	-2.7	-	0.30	2.2

[a] Basis is freshly prepared carbide before exposure to air; for reactivation, weight change was considered until 300 °C (Mo_2C) or 400 °C (W_2C)

[b] Basis is carbide after passivation and storage in a closed vial for 11 months at room temperature

[c] Using surface area of unpassivated carbide and metal atom density from carbide unit cell parameters

Attempts to passivate Mo_2C in H_2O or CO_2 are shown in Figure 3. As a reference to gauge the baseline oxygen content in the TG, the weight gain in argon flow at 300 °C is also presented. Exposure of the fresh Mo_2C sample to water vapor was initially carried out at 110 °C in order to discriminate chemical reaction of water with the carbide from adsorption of water. The sample gained 0.35% of its initial weight within two hours. However, when the water flow was stopped, the weight decreased by 0.21%, indicating that the weight gain was mainly due to weakly adsorbed water. When the sample was subsequently exposed to 16% O_2 at 40 °C, the sample weight increased at an initial rate of 4%/min and by 3% within 60 min, indicating that the sample was not passivated (Figure 3b). To further understand the interaction of water with the carbide surface, the temperature-programmed reaction experiment shown in Figure 4a was performed. The weight initially increased as the gas phase was switched from argon to a mixture of argon and H_2O at a temperature of 100 °C. Upon heating, the weight decreased as some of the water desorbed from the carbide surface, and then increased again as the sample was heated. Between 355 to 505 °C, the slow weight gain was accompanied by the evolution of carbon monoxide (m/z= 28). Above 505 °C, the weight gain accelerated. The MS traces of the gas phase showed a peak in the evolution of H_2 (m/z = 2) and carbon monoxide (m/z = 28) at about 600 °C. The formation of CO indicates that under these conditions the oxygen in the water molecule is removing carbon from the surface of the carbide.

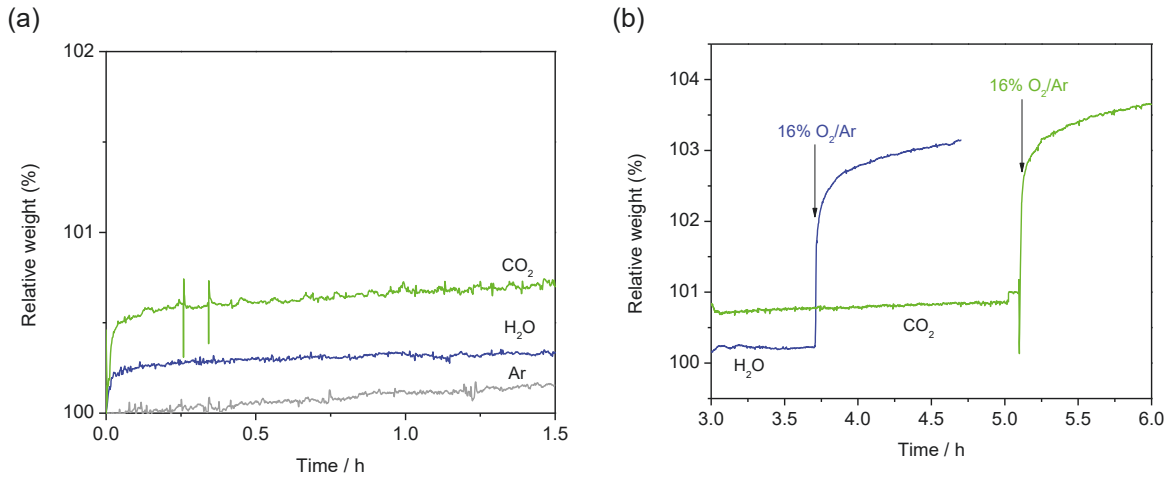

Figure 3: TGA of passivation of Mo_2C in various atmospheres at the specified temperatures: (a) 30% CO_2 at 100 °C, 1.8% H_2O at 110 °C, and Ar at 300 °C; (b) continuation with cooling to 40 °C and switch to 16% O_2/Ar.

Figure 3 shows that the exposure of Mo_2C to CO_2 at 100 °C resulted in a 0.7% weight gain within an hour. However, when the CO_2 flow was stopped, the weight decreased by 0.12%, indicating that some of the weight gain was due to weakly adsorbed CO_2. When the sample was subsequently exposed to 16% O_2 at 40 °C, the weight increased at an initial rate of 2.6%/min and in two hours the weight increase was 2.9%, indicating that the sample was not passivated.

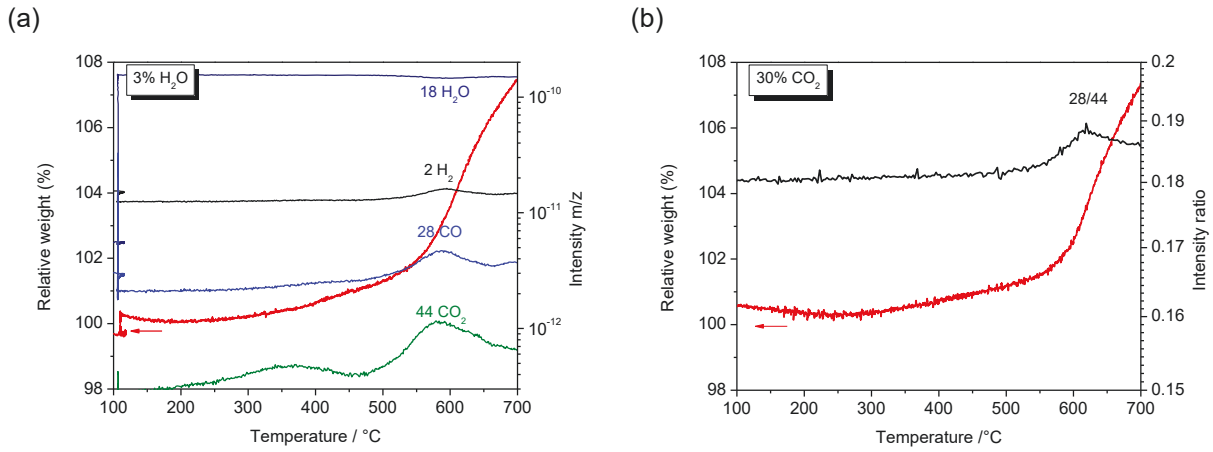

Figure 4: Weight change and effluent gas analysis by MS during temperature-programmed reaction of Mo_2C in various atmospheres (a) 3% H_2O and (b) 30% CO_2. Mass charge ratios and interpretation as labeled.

To further explore the ability of CO_2 to react with Mo_2C, a TP reaction experiment with 30% CO_2 was carried out (Figure 4b). When the sample was exposed to CO_2 at 40 °C and subsequently

heated, reversible adsorption of CO_2 was indicated by weight gain and subsequent weight loss (+0.7% and -0.3%). The onset for significant weight gain in 30% CO_2 was at about 580 °C, and at this temperature the formation of CO (m/z = 28) was observed. The rapid weight gain occurring at temperatures above 580 °C is consistent with bulk oxidation of the sample.

3.3. Reactivation of O_2-passivated carbides

Temperature-programmed reduction (TPR) was used to determine an appropriate regeneration temperature for the oxygen-passivated carbides. The reaction progress was followed by monitoring the evolution of water and methane, which were the only volatile products observed. The results of TPR in H_2 for the passivated Mo_2C samples are shown in Figure 5a. For the sample passivated using 1% O_2, the MS data show the loss of water starting at 20 min (155 °C) with a second, much smaller peak in water evolution as the sample reaches 700 °C. The only other gas phase product detected during the TPR experiments was methane (m/z = 16, 15). The sample passivated in 1% O_2 had a relatively large peak in methane formation with a maximum at about 540 °C. The sample passivated initially in 0.1% O_2 showed water evolution beginning at about 22 min (200 °C), and exhibited a relatively small peak in methane evolution with a maximum at about 68 min (625 °C).

To determine how effective passivation stabilized the Mo_2C carbide against oxidation, TPR was also performed with a Mo_2C sample that had been passivated in 1% O_2 and stored at room temperature in a closed vial for 11 months. Before reducing the carbide, the sample was heated in argon to 110 °C to remove physisorbed water. The results show that the sample stored for 11 months lost 9.7% weight compared to the 4.4% weight loss during TPR to 700 °C of a freshly passivated Mo_2C. Gas phase product analysis showed that the removal of oxygen reaches a maximum rate at 22 min (220 °C) for the aged sample, Figure 5a.

The TPR gas phase product traces for the W_2C samples are presented in Figure 5b. For both the 0.1 and the 1% O_2 passivated samples the total weight loss was about 5.9% after heating to 700 °C in 80% H_2. Similar to the Mo_2C sample, the W_2C sample showed only water and methane evolution during TPR. Both W_2C samples show two peaks in water evolution with maxima at about 20 and 35 min (125 and 275 °C). Methane evolution started at 55 min (510 °C) and increased sharply at 70 min (640 °C) independent of the passivation procedure.

(a)

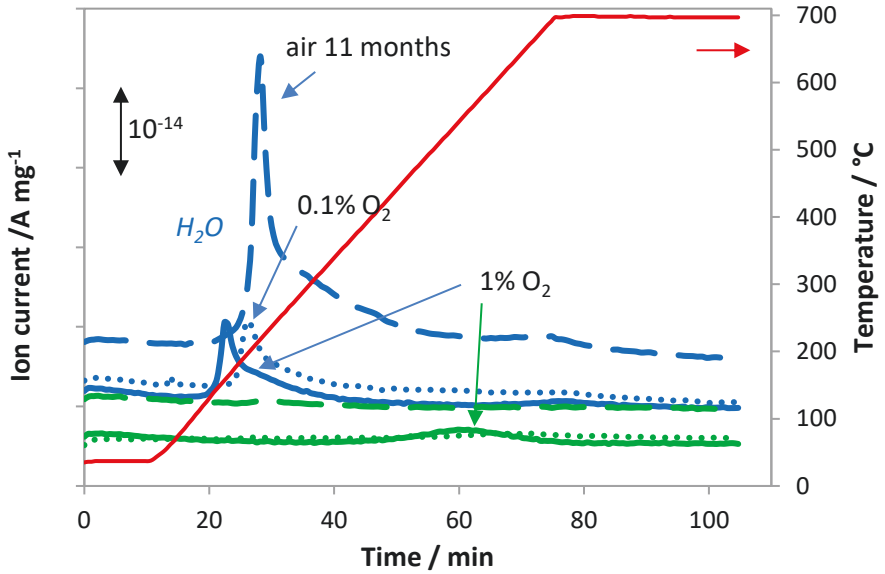

(b)

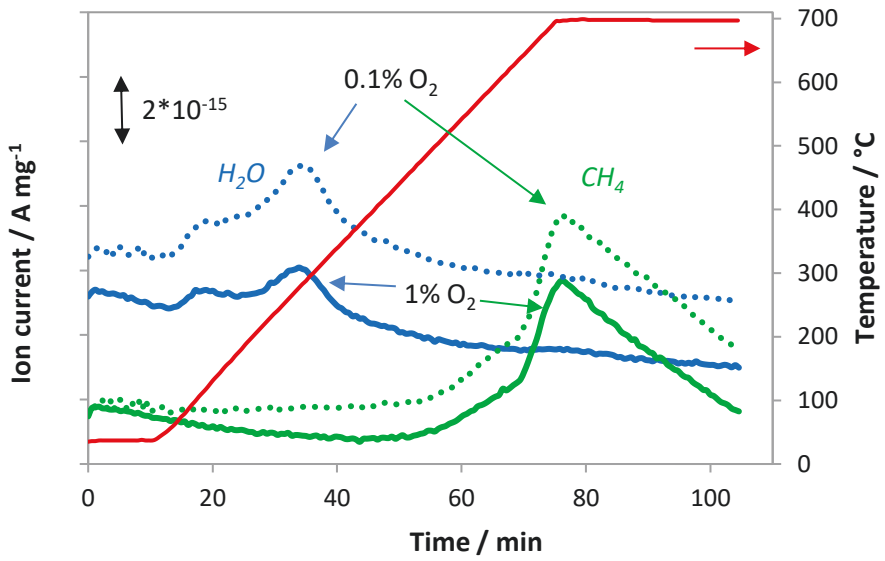

Figure 5: Effluent gas analysis by MS during temperature-programmed reactivation in H_2 of (a) Mo_2C and (b) W_2C. Solid lines - passivated in 1% O_2; dotted lines - passivated in 0.1% O_2; dashed lines - Mo_2C passivated in 1% O_2 and stored for 11 months. Water - blue curves (m/z=18), methane - green curves (m/z=15). Gas flow of 50 ml/min 80% H_2 in Ar.

The TPR data were used to select the regeneration temperatures for both catalysts. The criteria were that the temperature was high enough to remove the oxygen that was added during passivation, but low enough to not remove carbon (as methane) from the surface. For the Mo_2C samples, the regeneration temperature was 300 °C (35 min on Figure 5a) and for the W_2C samples, the regeneration temperature was 400 °C (46 min on Figure 5b). At these temperatures, the mass of the carbides was nearly that prior to passivation (Table 2). To corroborate the success of the reduction procedure, the surface sites were probed by CO chemisorption after removal of the oxide layer in H_2. The results, shown in Table 3, indicate an excellent recovery of the surface sites for Mo_2C after passivation in 0.1% O_2, and only a small loss of around 10% of sites after passivation in 1% O_2. The passivation and subsequent reduction treatments affected the W_2C surface more than the Mo_2C surface, but the recovery of sites was still good at 82-86%.

Since hydrogenations are often conducted at elevated pressure, the TP reaction of passivated and unpassivated carbides with H_2 at 20 bar was investigated (Figure 6). At this pressure, methane evolution from Mo_2C was already observed at a temperature of about 300 °C, independent of prior passivation. In contrast to this behavior, previously passivated W_2C released more methane than in-situ prepared W_2C and in two consecutive steps rather than in a single event.

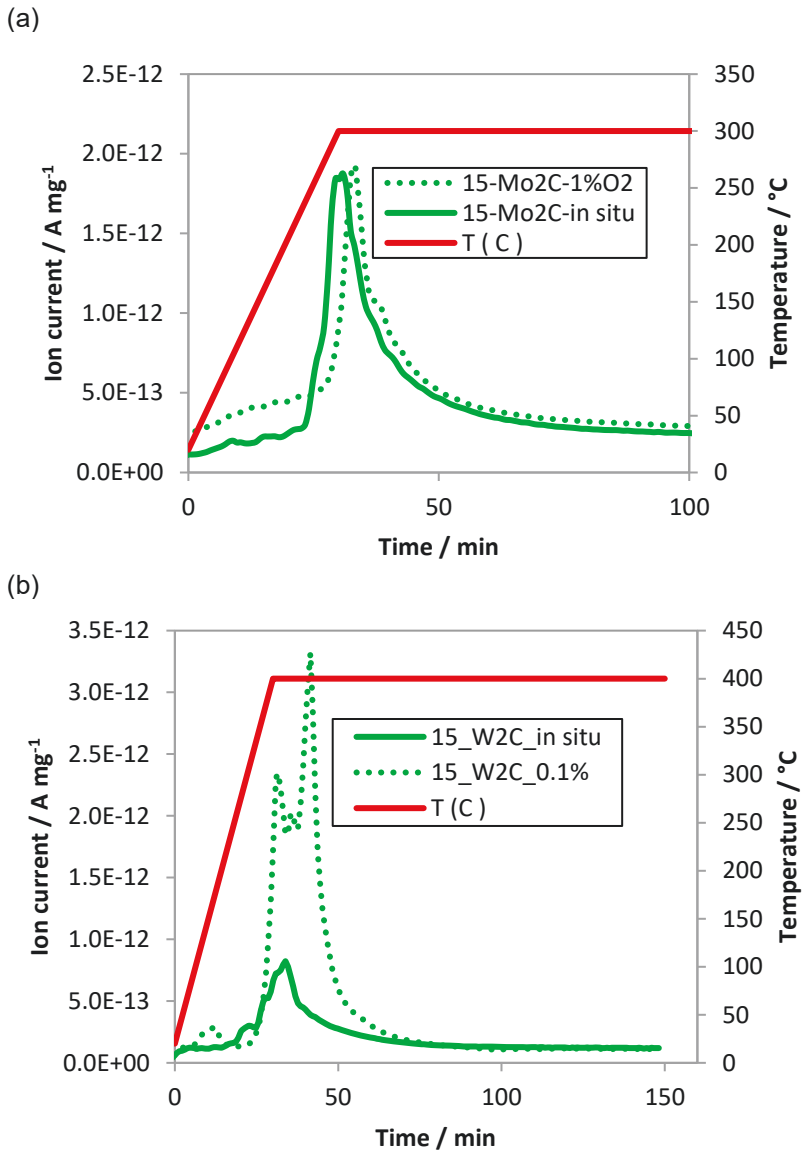

Figure 6: Effluent gas analysis by MS during reduction of unpassivated and passivated carbides with H_2 at 20 bar. Traces represent m/z=15 (methane). (a) Mo_2C, in situ synthesized and 1% O_2 passivated and (b) W_2C in situ synthesized and 0.1% O_2 passivated

To test whether the original carbidic state could be restored in the carburization mixture, an additional TPR experiment was carried out with the 1% O_2 passivated Mo_2C sample using a combination of H_2 and ethane. The gas phase products of this TPR are presented in Figure 7. The samples were heated at 5 °C/min in 10% C_2H_6 in H_2 to the final carburization temperature of 650 °C. Gas phase analysis shows water formation starting at 100 °C with the maximum at 120 °C, and hydrogenolysis of ethane to form methane began at 350 °C.

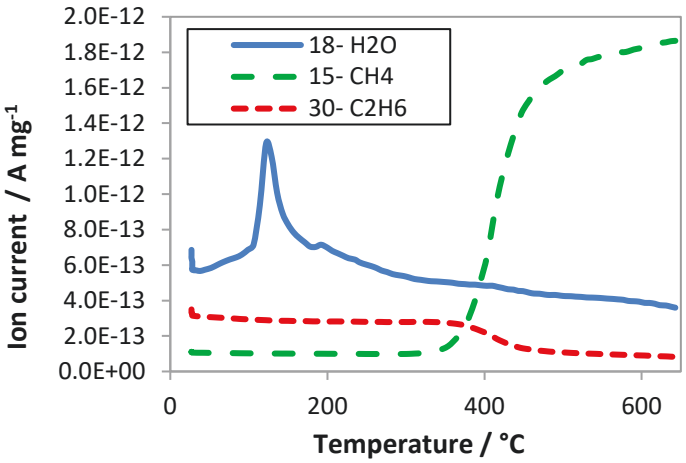

Figure 7: Effluent gas analysis by MS during reactivation of passivated Mo_2C (1% O_2) with the carburization mixture of 10% ethane in H_2.

3.4. Catalytic activity

Hydrogenation of toluene (20 bar, H_2: toluene = 33) was used to test the catalytic activity of the carbide samples. The Weisz-Prater criterion was applied to exclude mass transfer limitations (see the supporting information). The rate of conversion on samples that were synthesized ex situ, passivated and transferred into the reactor and then reduced was compared to that on "fresh" samples that were synthesized in situ (in the reactor) and not passivated or contacted with air. The hydrogenation activity of in situ-prepared Mo_2C is compared with that of 0.1% and 1% O_2 passivated and reduced samples in Figure 8. The only product detected at a temperature of 150 °C was methylcyclohexane, and the data show that the fresh sample and the 0.1% O_2 sample had the same rate of conversion, but the conversion at 150 °C was about 30% lower for the 1% O_2 passivated sample. The 1% O_2 passivated sample that was reduced in the carburization mixture (650 °C, 10% ethane in H_2 at 1 bar) showed somewhat better activity than the sample reduced in H_2 at 300 °C, but still lower than the fresh sample. Reduction at 20 bar of H_2 resulted in a lower activity that could not be recovered through further treatments. After collecting data at 150 °C, the catalysts were tested at 200 and 300 °C. The product distribution at the higher temperatures was dominated by light alkanes. The catalysts were then cooled to 150 °C to determine whether any deactivation had occurred during operation at higher temperature. Surprisingly, the catalysts that were used for toluene hydrogenation at higher temperature were significantly more active at 150 °C than they were directly after reduction.

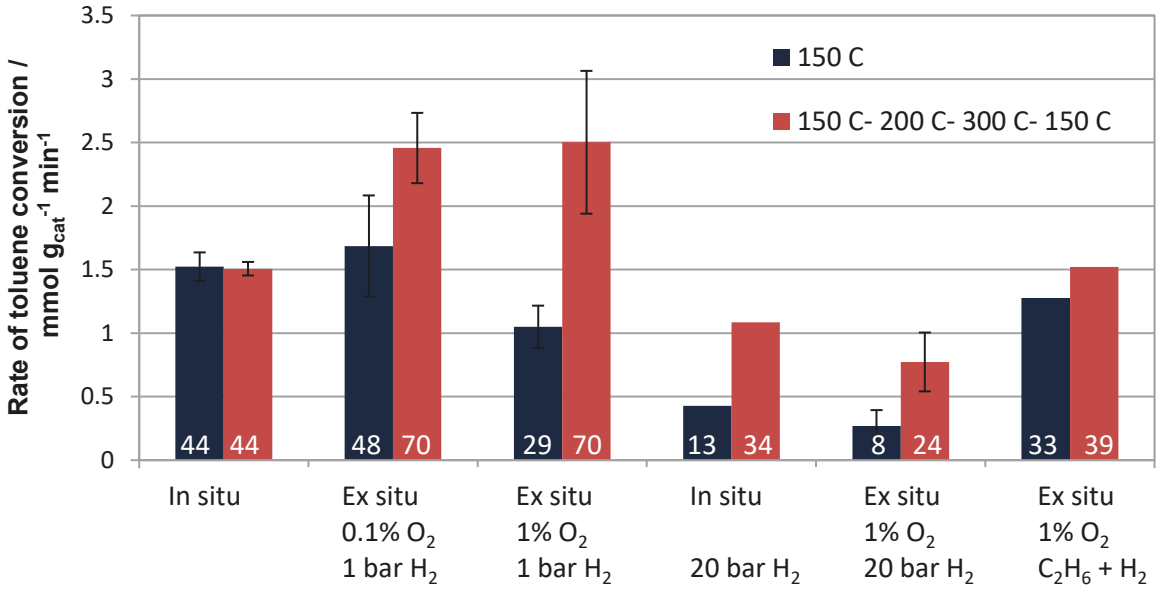

Figure 8: Hydrogenation of toluene on Mo_2C, steady state rates. Total pressure 21 bar, H_2/toluene = 33, WHSV = 20 g/(g_{cat} × h). Dark blue: initial activity at 150 °C; solid red are activity at 150 °C after use at higher temperature (1.5 h, sequentially, at 150, 200 and 300 °C). Error bars are standard deviations for complete reproduction (different carbide batch). Conversions are given in % at the bottom of each bar.

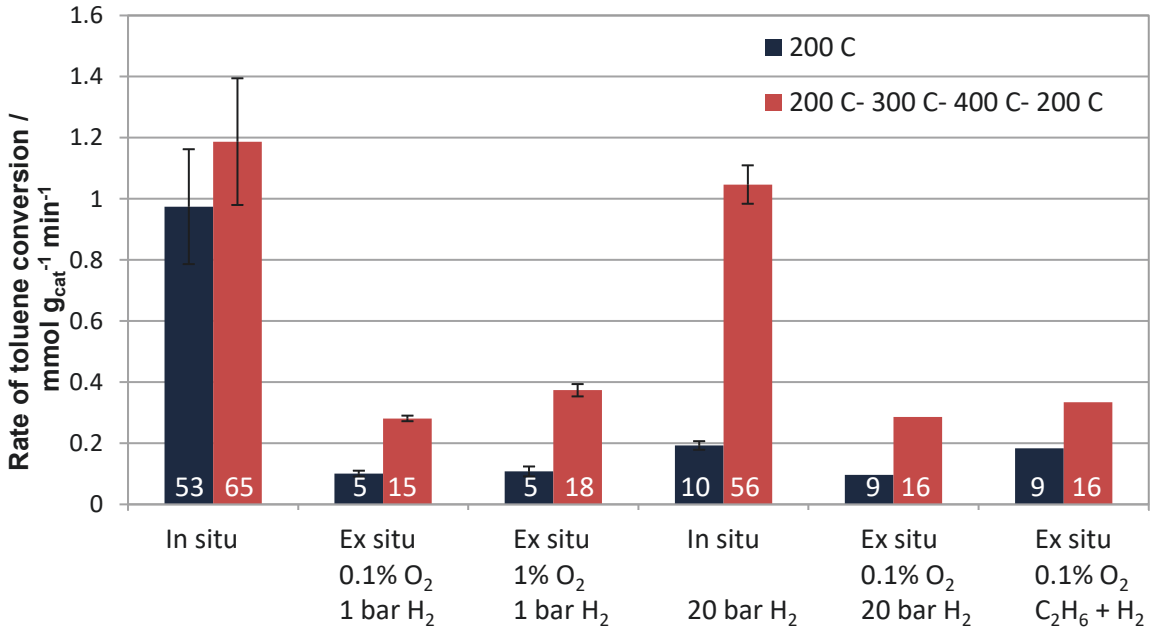

Figure 9: Hydrogenation of toluene on W_2C, steady state rates. Total pressure 21 bar, H_2/toluene = 33, WHSV= 10 g/(g_{cat} × h). Dark blue: initial activity at 200 °C; solid red: activity at 200 °C after use at higher temperature (1.5 h, sequentially, at 200, 300 and 400 °C). Error bars are standard deviations for complete reproduction (different carbide batch). Conversions are given in % at the bottom of each bar.

Table 3: Measured and reported toluene ring hydrogenation rates of carbides and noble metals in relation to surface area and number of sites

Material [Ref.]	*Description*	*Surface area[a] m^2/g*	*Sites[a] µmol/g*	*Temp. °C*	*P(toluene) bar*	*P(H_2) bar*	*Tol. Conv. %*	*Rate mmol m^{-2} h^{-1}*	*Est.TOF s^{-1}*
Mo_2C (*hP*3) [this work]	Fresh, steady state	58	15.8[b]	150	0.57	20.43	44 ± 0.03	1.58	1.61
	0.1% O_2 pass./ H_2-red. steady state		15.5[b]	150	0.57	20.43	48 ± 13	1.74	1.81
	1% O_2 pass./ H_2-red. steady state		14.5[b]	150	0.57	20.43	29 ± 5	1.09	1.21
"β-Mo_2C" [31]	initial activity	12-15		150	0.69	30	100[c]	1.39	
	steady state			150	0.69	30	20[c]	0.28	
Mo_2C (hex.) [32]	initial activity	5.2		150	0.01	4.79	45	1.09	
	steady state			150	0.01	4.79	7	0.17	
Mo_2C (fcc) [33]	From unpressed MoO_3	2.3		150	27.6[d]		2.3	0.17	
	From pressed MoO_3	4.2		150			36.1	1.49	
Mo_2C_{1-x} (and MoO_2) [37]	WHSV = 0.35 h^{-1}	12.7		150	27.6[d]		26[c]	0.08	
	WHSV = 1.60 h^{-1}			150			2.5[c]	0.03	
W_2C (*hP*3) [this work]	Fresh, steady state	35	8.7[b]	200	0.57	20.43	53 ± 12	1.67	1.87
	0.1% O_2 pass./ H_2-red. steady state		7.5[b]	200	0.57	20.43	5 ± 1	0.17	0.22
	1% O_2 pass./ H_2-red. steady state		7.1[b]	200	0.57	20.43	5 ± 2	0.18	0.25
Pt/HZSM-22 [34]	0.5 % Pt, 30% dispersion		2000	150	0.20	1[c]			0.10
				150	0.20	2[c]			0.20
Pt/C [35]	4.7 wt% Pt, d=5.42 nm	19[e]	518[e]	150	0.17	0.83	92.5	54.26	0.58
Pd/C [35]	5.4 wt% Pd, d= 5.95 nm	28[e]	783[e]	150	0.17	0.83	2.8	0.96	0.01
Ru/C [35]	4.0 wt% Ru, d=4.57 nm	47[e]	1360[e]	150	0.17	0.83	10.7	2.98	0.03

[a]surface area of carbide or metal; sites per gram carbide or gram metal
[b]from CO chemisorption
[c]read from graph
[d]total pressure
[e]calculated from specified metal particle size (from transmission electron microscopy), using bulk metal density and assuming spherical particles and one site per surface atom

Figure 9 shows the toluene conversion results for W_2C, which was generally much less active than Mo_2C, requiring a higher reaction temperature of 200 °C. Unlike the Mo_2C sample, the W_2C sample had a much lower conversion rate after passivation in either 1% or 0.1% O_2 followed by reduction in H_2 at 1 or 20 bar at 400 °C. The sample that was regenerated at 700 °C in the carburization gas showed only slightly better activity than that reduced at 400 °C. During toluene hydrogenation at up to 400 °C (1.5 h, sequentially, at 200, 300 and 400 °C), almost all samples became more active; however, if they had ever been passivated in O_2 the activity remained significantly below that of the fresh sample (data in solid red).

The toluene ring hydrogenation rates of fresh and of passivated and reactivated carbides were related to surface area and to the number of sites as determined by CO adsorption, Table 3. The surface area-related rates and turnover frequencies (TOFs) slightly decreased in the case of Mo_2C after passivation in 1% O_2 and reactivation whereas they dramatically decreased in the case of W_2C after either type of passivation and reactivation.

4. Discussion

4.1. Carbide characterization

XRD data demonstrate that the materials produced are Mo_2C(*hP*3) and W_2C(*hP*3), characterized by hexagonally close packed metal atoms and carbon in the octahedral gaps. Further distinction into two different structures, as suggested by the match with the ICDD powder diffraction files, is not supported by the XRD data in Figure 1. The difference between the two structures lies in the random or ordered distribution of carbon in the octahedral gaps of the close packings, and the effect on the diffractograms is so subtle that a distinction cannot be made. More importantly, the diffractograms are analogous to those published by Oyama et al. [36] and Hanif et al. [11] for Mo_2C prepared by temperature-programmed reaction and to that published by Xiao et al. [6] for W_2C. There is some confusion regarding the traditional Greek letter nomenclature of these phases. The powder diffraction files specify α-Mo_2C and α-W_2C as alternate names. However, the name α-Mo_2C is also associated with several reported orthorhombic structures (ICDD # 00-031-0871, 01-071-0242, and 01-089-2669) and has been used for fcc Mo_2C [37]. Some authors [38] have proposed to follow a convention defined by the ICDD and refer to hexagonal Mo_2C as α-Mo_2C and to orthorhombic Mo_2C as β-Mo_2C. In light of these conflicts, it appears best to adhere to the IUPCA recommendation of the Pearson symbol *hP*3 and to emphasize

that the observed phases are consistent with previously reported high-surface area hexagonally close packed structures designated as β-Mo_2C and β-W_2C in the catalysis literature [2,11]. The bulk structure of the carbides is retained after passivation.

The total weight loss during synthesis was 28.5% and 17.8% for molybdenum and tungsten carbides, respectively. These weight losses are slightly lower than expected for the carbide stoichiometry of $MeC_{0.5}$ (Me=Mo or W) that is indicated by the XRD data. This result also demonstrates that mass losses through volatilization of molybdenum were insignificant and that extraneous carbon or oxygen is present in the samples. Deposition of surface carbon, which typically starts after carbide formation, is associated with a pronounced increase in weight and was avoided by terminating the carburization process before any such weight gain occurred. It is more likely that there is some remaining oxygen in the carbides. The diffractograms show relatively broad peaks consistent with very small crystalline domains, or with a disordered structure that could be indicative of occluded oxygen. The inflection point in the weight loss trace observed during synthesis of both carbides was consistent with the formation of the metal dioxide as an intermediate in the synthesis (measured weight loss of -11.2% vs. calculated loss of -11.11% for MoO_3 to form MoO_2, and -7.0% vs. -6.9% for WO_3 to form WO_2). These results are in agreement with observations in the literature of intermediate MoO_2 [10] and WO_2 [6] formation.

The BET surface areas of the carbides before passivation were 58 m^2/g and 35 m^2/g for Mo_2C and W_2C, respectively. After passivation in 1% O_2, the surface areas decreased by 26% and 34% to 43 m^2/g and 23 m^2/g for Mo_2C and W_2C, respectively. This decrease in surface area was accompanied by a decrease in pore volume and an increase in the mean pore size, both indicating a closing or blocking of smaller pores. A loss in surface area upon passivation is consistent with the literature; for example, Rocha et al. found initial surface areas of 94 m^2/g reduced to 25 m^2/g after passivation overnight in 0.5% O_2 [16]. The surface areas of the 1% O_2 passivated materials are equal or slightly lower than those reported in the literature for 0.5% O_2 passivated materials [2], suggesting that mild passivation conditions are favorable for maintaining surface area.

4.2. Passivation procedures and their effectiveness

Mo_2C and W_2C can be passivated with oxygen at room temperature. In recent literature, passivation with 1% O_2 at room temperature is the most common passivation method. Here, the

effect of passivation in oxygen at both 0.1% and 1% O_2 was investigated to determine if there is an advantage to passivation at lower O_2 concentrations.

The weight gains during passivation with 1% O_2 and with, initially, 0.1% O_2 are significantly different for Mo_2C, but not for W_2C, Table 2. The majority of the weight gain and associated heat evolution happened during the first thirty minutes of the passivation with both oxygen concentrations. Using the lower O_2 partial pressure decreases the initial rate of weight gain by 7 times in the case of Mo_2C and 6 times for W_2C. The rate of oxygen addition to Mo_2C is 0.15 and 1.08 mol O_2/g_{cat} h for 0.1% and 1% O_2, respectively. Because no gas phase products were observed during passivation, the weight gain can be directly related to oxygen addition. For Mo_2C, the passivated carbides adsorbed 1.7 oxygen/surface metal atom for 1% O_2 passivation and 1.5 oxygen/surface metal atom for 0.1% O_2 passivation. The heat of reaction for the oxygen addition to Mo_2C is estimated to be 170 to 200 kJ/mol oxygen. While the coordination of oxygen on these passivated samples is not known, DFT calculations on β-Mo_2C have indicated that the different surface planes have different reactivities toward oxygen chemisorption, and that they can adsorb different amounts of oxygen. At less than 1 L exposure, oxygen prefers to adsorb on top of Mo atoms, and for increasing coverage, oxygen atoms start to adsorb on hollow sites between Mo atoms that are not occupied by carbon atoms [39,40]. The observed stoichiometry can be explained with oxidation of the top layer only, but migration of oxygen into subsurface layers cannot be excluded. The sharp exotherm seen at the higher O_2 concentration implies locally higher temperatures and possibly increased ion mobility. The slightly higher oxygen uptake of W_2C of about 2.2 oxygen/surface metal atom may be ascribed to the higher oxophilicity of this transition metal.

Evidently, the main advantage of a lower O_2 concentration is better control of the sample temperature, which is associated with less weight gain, implying that oxidation is confined to the surface. Regarding these observations, it must be considered that the physical configuration of the sample will influence the heat transfer away from the sample, and thus the oxidation rate for any particular O_2 concentration. Here, a very small amount of sample (ca. 40 mg) in an alumina crucible of somewhat greater mass was used. A considerable increase in the sample mass or decrease in heat removal rate could require even lower O_2 concentrations, periodic O_2 additions with added time for cooling, or lower gas flow rates per gram catalyst.

To check whether passivation is effective and samples can be exposed to the ambient without further change, the concentration of oxygen was increased to 16% for 1 h. The rate of weight gain was not significant for Mo_2C in both cases, indicating that the samples were no longer pyrophoric and may be briefly exposed to air for a transfer. The slow continued weight increase implies that full passivation requires long exposure times. It has been reported that oxygen is very mobile in Mo_2C and that oxygen will diffuse into Mo_2C if it is exposed for several weeks at room temperature [41]. Consistent with these reports, the additional oxygen uptake of an already passivated Mo_2C sample during storage in the laboratory for 11 months was significant. The weight loss during reduction was 9.7% (Table 2), indicating that the "passivated" samples are not stable in air over extended periods.

The limitations of O_2 passivation, in particular the difficulty to control the extent of oxidation, have promoted the search for other agents, and CO_2 and H_2O have been advertised as milder passivation agents [22], with DFT calculations suggesting that bulk oxidation is not favorable [42]. The isothermal passivation data in Figure 3a indicate that H_2O and CO_2 adsorb on the carbide surface at 110 and 100 °C, respectively. However, the adsorption is partially reversible and the subsequent exposure of the surface to 16% O_2 at 40 °C results in a rapid weight gain, indicating that the samples are not passivated (Figure 3b). This result is in conflict with reports in the literature that H_2O and CO_2 can passivate Mo_2C at room temperature, and that CO_2 can passivate mixed nitrides or carbides at temperatures below 400 °C [22,23]. TP reaction experiments (Figure 4a) indicated that the reaction of water with the Mo_2C surface commences at 505 °C and results in the removal of carbon from the carbide surface as CO, making water unsuitable as a passivation agent at any temperature. The TP reaction experiments with CO_2 show that significant weight gain and reaction with the surface of the carbide begin at about 580 °C with the production of CO and presumably oxidation of the carbide surface, Figure 4b.

Dissociation of CO_2 on supported Mo_2C has also been reported in the literature as requiring temperatures higher than 550 °C [43]. Darujati et al. have reported that β-Mo_2C was stable up to 600 °C (by XRD) in 0.25 bar H_2O or CO_2, but at higher temperatures, bulk oxidation to MoO_2 occurred [44]. Certainly, these temperatures are too high to allow only surface interaction. The final synthesis temperature of Mo_2C is only 50 °C higher, and clearly, bulk diffusion is facile at this temperature. There are literature reports from Porosoff et al. that show CO formation at less

than 250 °C from a mixture of CO_2 and H_2 on Mo_2C [45], or from Nagai et al. that show reduction of CO_2 in H_2 at 300 °C with supported molybdenum carbides [46]. However, it has been shown that the presence of H_2 is key to this low temperature activation of CO_2 (DFT) [47].

In conclusion, neither H_2O nor CO_2 reacts with the fresh carbide surface at mild temperatures to form a stable and passivating layer; and reaction initiation occurs only at unfavorably high temperatures that also permit reaction of the carbide bulk.

4.3. Reactivation of passivated carbides

If the catalytic properties of the carbide itself are desired then the oxide layer on the surface of the carbides must be removed. Oxygen can be removed either by temperature-programmed desorption (TPD) or TPR using H_2. With TPD, the oxygen will react with carbon in the carbide structure and leave as CO or CO_2 [41,48-50]. TPR with H_2 removes the oxygen as water. Because removal of oxygen by TPD damages the carbide and requires high temperature, this method was not investigated.

It is expected that the temperatures for oxygen removal by H_2-TPR may be affected by location of the oxygen at the surface or in the bulk, by the redox potential depending on the nature of the metal and its valence, by the ability of the surface to activate H_2, and by experimental parameters such as heating rate.

Leary et al. reported two peaks of water in the reduction of an air exposed Mo_2C (4 m^2/g), a first, sharp peak at about 200 °C that they attribute to surface oxygen and a second peak at about 300 °C attributed to oxygen diffusing from bulk to surface [25]. The data in Figure 5 show a single peak shifted to lower temperature, consistent with the removal of surface oxygen at a much lower heating rate (5 °C/min vs. 60 °C/min). No second maximum in water desorption could be discerned below 300 °C, but rather a broad tail in water desorption was observed, which was particularly prominent for the sample stored for 11 months. The lack of a distinct 2nd peak suggests the absence of bulk oxygen, and the much higher surface area of the samples investigated here in comparison to those investigated by Leary et al. implies that surface oxygen should be predominant. Methane formation from Mo_2C was significant only at high H_2 pressure (Figure 6), that is, at high hydrogen and low carbon chemical potential in the gas phase.

Effects of the passivation conditions were subtle. The Mo_2C sample passivated in 1% O_2 was not only characterized by the lowest water formation temperature but also by the most pronounced methane formation and the lowest methane formation temperature, indicating the least stable surface and a possible relationship between the loss of carbon and shift in water desorption temperature. Surprisingly, the sample stored for 11 months, which contained the highest concentration of oxygen, did not lose carbon in the form of methane during TPR.

For W_2C, no significant difference can be seen between reduction of W_2C passivated in 0.1 or 1% O_2. In both cases, there are two water peaks. The first peak is assigned to removal of oxygen from the surface or from more highly oxidized tungsten. The second peak could be due to removal of oxygen from less highly oxidized tungsten, or from below the surface. Both samples desorb methane during the TPR starting at about 475 °C in amounts that are more significant than those released from Mo_2C, indicating a comparatively lower stability of the tungsten carbide surface.

It was hypothesized that complete removal of the oxygen should restore the catalytic performance of the original carbide provided that no other changes are inflicted. The TPR profiles (Figure 5), independent of the transition metal and the passivation procedure, show a time gap between water and methane evolution, that is, a temperature window exists that allows oxygen removal without loss of carbidic carbon. Moreover, the weight loss during reactivation corresponds to the weight gain during passivation (Table 2), demonstrating that oxygen removal is complete at 300 or 400 °C for Mo_2C or W_2C, respectively. Some papers have suggested other reduction temperatures for Mo_2C (700 °C [44] or 450 °C [45]) or W_2C (300 °C [51]); the difference in suggested reduction temperature could be due to different synthesis methods. For example, some synthesis methods could result in the deposition of carbon on the surface that would then need to be removed by applying higher reduction temperatures (*e.g.*, 600 °C [10]).

4.4. Surface sites and catalytic behavior

The surface properties and the effectiveness of the various passivation and reactivation procedures were assessed by measuring CO adsorption capacity and toluene hydrogenation activity. In Table 3, these results are compiled and contrasted with information from the literature.

CO adsorption capacity of carbides is known to vary depending on carbide structure and preparation conditions, for example from 16.7 μmol/g for slightly carbon-deficient hcp Mo_2C [52]

to 208 μmol/g for not completely phase-pure fcc Mo_2C []. The CO uptake of W_2C can vary in a similar range [54]. While there is some correlation of CO uptake with surface area, the site density can still extend over two orders of magnitude [55]. Both fresh Mo_2C and fresh W_2C exhibited CO uptakes at the lower end of the reported range at 15.8 and 8.7 μmol/g, respectively.

Comparison of the catalytic performance of in situ prepared samples with literature data is not straightforward because of some differences in reaction conditions combined with incomplete knowledge of the rate law. Data for toluene hydrogenation on Mo_2C at a temperature of 150 °C are available, and the reaction is 100% selective to methylcyclohexene, consistent with the observations in this work. For the reports cited in Table 3, toluene and H_2 pressures differ from the conditions in this work. Knowing the toluene pressure dependence is principally critical not only because of the spread from 0.01 to 0.69 bar in the cited data, but also because most catalytic data were collected at non-differential conversions that reach up to 100%. These concerns can be alleviated through the report by Frauwallner et al. [37], who found the ring hydrogenation to be zero order in toluene on a (not phase-pure) Mo_2C catalyst, consistent with observations made with noble metal catalysts [56]. There is no information on the toluene hydrogenation reaction order in H_2 on transition metal carbides. Toluene hydrogenation on noble metals has been found to be first order in H_2 at subatmospheric pressures [57], and a similar pressure dependence cannot be excluded for carbides. Fortunately, all investigations of carbides in Table 3 were conducted in large H_2 excess, and it can be reasoned that H_2 conversions were differential. None of the literature reports on carbides contained both CO adsorption and toluene hydrogenation data, and, hence, the rates were related to surface area to allow comparison (second-to-last column in Table 3). Given the different preparation methods and conditions, the surface-related rates are surprisingly similar, only the MoO_2-containing Mo_2C sample of Frauwallner et al. [37] is significantly less active. W_2C reaches rates comparable to those seen with Mo_2C only at 50 °C higher temperature.

For supported noble metal catalysts, generally more information is available; for example, the number of accessible platinum sites [34] or the particle size [35], which can be used to estimate metal surface area and the number of the surface sites. The reaction is more than 95% selective to methylccylohexane [34,35]. Noble metals are generally characterized by a much higher site density than carbides. As a result (not accounting for differences in reactant partial pressures which may affect the reaction rates), the estimated TOFs for carbides and noble metals are in the same

order of magnitude whereas the surface area-related rates differ. The TOFs have to be considered with some caution, because, at least on noble metals, the reaction is structure-sensitive [56,58], suggesting an ensemble site.

Finally, it is useful to contrast catalytic performance and CO uptakes after passivation and reactivation. Figure 8 shows that the original activity of Mo_2C can be recovered if the 0.1% O_2 passivation procedure is applied and the material is reactivated by reduction in H_2 or re-carburization. These data also prove that the reduction procedure optimized on the basis of TG data can be reproduced in the reactor. Further confirmation of complete restoration comes from CO adsorption, which showed nearly the same number of sites as for the fresh sample (Table 3).

A different picture evolves for Mo_2C passivated with 1% O_2, whose activity could not be completely restored by reduction or recarburization. The activity declined more than the CO adsorption capacity (31% vs. 9%), indicating that the quality of the sites changed. For W_2C, activity after passivation and reduction or recarburization was far below that of a fresh sample, with only a small effect for changes in the conditions of any of the reactivation steps (Figure 9). Even at an 80% recovery of the CO adsorption capacity (Table 3), toluene hydrogenation activity of W_2C was insignificant. Hence, the quality of the sites must change. Such variations in carbide surface properties are principally consistent with data published by Lee et al. [59], who reported a spread in average turnover rate for benzene hydrogenation on differently prepared molybdenum carbides.

The disparity between CO adsorption capacity and toluene hydrogenation rates could have several causes. The reason for the decline in activity is probably not a loss of the ability to activate H_2, for two reasons. H_2 and CO adsorption on carbides have been found to give consistent results [60], implying that CO uptake is also a measure of sites for H_2 activation. Also, H_2 is readily activated by the passivated surface during reduction of passivated carbides at atmospheric or elevated pressure (Figure 5 and Figure 6). Hence, the decline in activity is likely associated with toluene access to the sites, or its adsorption and activation. CO is smaller than toluene and could probe more sites than are accessible for toluene adsorption, but it seems unlikely that this difference would account for the total loss of activity of W_2C after passivation and reduction. Residual oxygen would be another possibility, which would weaken the binding energy of carbon much more than that of hydrogen according to DFT calculations [42] and could thus account for a

change in ring hydrogenation activity. However, the near quantitative removal of the oxygen deposited during passivation (Table 2) speaks against this scenario. Another possible explanation for the activity loss of Mo_2C and W_2C is that ensemble sites needed for toluene activation lose their integrity during passivation and reactivation. Support for this hypothesis comes from the oxygen-to-metal ratios after passivation (Table 2). Assuming Me=O and Me-O-Me surface moieties (with Me = Mo or W) are formed on coordinatively unsaturated metal sites, low concentrations of oxygen can be accommodated on top of the surface without incorporation of oxygen into surface or subsurface layers. Oxygen-to-metal ratios of two and higher, as seen for W_2C, imply disruption of tungsten-tungsten coordinations in the surface layers, resulting in a defective surface after reduction. To capture such a change, it may be useful to apply other probes (such as toluene itself) in addition to CO to characterize carbide surfaces.

4.5. Carbide surface dynamics

The toluene hydrogenation activity of the catalysts at 150 °C (Mo_2C) or 200 °C (W_2C) was found to be increased after operation at higher temperatures, except for the in situ prepared samples. The increased activity indicates a change to the catalyst surface, and the following possibilities were considered: removal of oxygen left from the passivation, removal of carbon, addition of carbon to the carbide surface, restructuring of the carbide surface.

Removal of residual oxygen as a cause for the activity increase was excluded because the weight loss during TPR at 1 bar H_2 corresponds to the weight gain during passivation, and because TPR experiments to 700 °C at 1 bar H_2 (Figure 5) show no additional water formation events that could be shifted to lower temperatures at increased H_2 pressure. While oxygen is cleanly stripped from Mo_2C using 1 bar H_2 with good recovery of the activity of the original carbide, there is an irreversible effect of oxygen on W_2C. The higher oxygen-to-metal ratio after passivation (2.2 vs. 1.5 to 1.7) indicates penetration of the oxygen into deeper layers and possible disruption of the surface.

Removal of carbon was clearly promoted by high pressure H_2, as shown by reduction experiments with in-situ prepared and with passivated samples at 20 bar H_2 at 300 °C (Mo_2C) or 400 °C (W_2C) (Figure 6). Methane evolved at much lower temperatures than when 1 bar H_2 was used. The loss was transient, implying that only carbon on or near the surface reacted or that all carbon was removed. The carbon removal was not beneficial (Figure 8, Figure 9); the carbon-

depleted samples were characterized by low toluene hydrogenation activity at 150 °C (Mo_2C) or 200 °C (W_2C).

The twofold or more enhancements in activity of the harshly reduced and thus carbon-depleted samples after operation at higher temperatures indicates that addition of carbidic carbon to the surface is occurring. In fact, it has been reported that increasing the amount of carbidic carbon on a Mo_2C surface increased the hydrogenation activity of Mo_2C by increasing both the number and quality of the active sites [61]. While the original activity was recovered when in situ synthesized W_2C was reduced at 20 bar H_2 and intermittently operated at 400 °C, the recovery for Mo_2C was not perfect, likely because the maximum temperature of 300 °C applied during toluene hydrogenation does not allow for enough mobility for recarbidization and restructuring.

Presumably, carbon removal from the carbide is also possible at high temperature and 20 bar H_2 when toluene is present, but the anion deficiency is apparently compensated with carbon from toluene and the resulting surface behaves like a carbide. For W_2C previously reduced at 20 bar H_2, surface recarbidization was evident through a change in selectivity at 400 °C from dealkylation to hydrogenolysis with time on stream; initially benzene was observed and later light alkanes as for the other samples. The chemistry can be considered as analogous to hydrodesulfurization [62] or hydrodenitrogenation [63] in that a surface anion vacancy is filled with a main group element, only the chemical potentials must be balanced such that incorporation of the element is favored over formation of the volatile hydrogen compound (i.e., methane in this case).

O_2-passivated samples also experienced enhancement through reduction and conditioning in the feed. One conclusion from this data is that carbide synthesis is possible at much lower temperature than typically employed (≥ 300 °C lower than needed during atmospheric pressure synthesis). The H_2 pressure needs to be high enough to remove oxygen from the precursor and a sufficiently reactive carbon source must be available. Such a synthesis may be useful for in situ formation of carbides if a reactor is designed for high pressure but not high temperature. An interesting and curious result that merits further investigation is the higher activity of the passivated and feed-conditioned Mo_2C materials over a freshly prepared carbide.

5. Conclusions

Various agents and methods for the passivation and regeneration of Mo_2C and W_2C have been investigated. Contrary to previous reports, water and carbon dioxide were found to be unsuitable for passivation of Mo_2C or W_2C. Water reacted with the carbide surface only at 505 °C, and then it removed carbon from the surface at this temperature. Carbon dioxide needed a temperature of 580 °C to dissociate on the surface of molybdenum carbide. At lower temperatures, neither water nor carbon dioxide adsorbed strongly enough to passivate the carbide surfaces.

When passivating Mo_2C with O_2, a mild passivation with an initial O_2 concentration of 0.1% produced a more active catalyst after reduction when compared to the more commonly reported procedure of passivation with 1% O_2. Regeneration of a 0.1% O_2 passivated samples by reduction at 1 bar H_2 and 300 °C for 2 h was sufficient to regain activity equivalent to that of an unpassivated sample. For the 1% O_2 passivated sample, recovery of the original hydrogenation activity required treatment in the carburization gas at 650 °C, the initial synthesis temperature.

Passivation in O_2 is not sufficient to protect the Mo_2C samples from further oxidation. Over 11 months at room temperature, a passivated sample continued to react with atmospheric oxygen and contained 2.8 times as much oxygen as the fresh sample gains during passivation. This observation has two implications; passivated Mo_2C samples will have a shelf life under ambient conditions, and storage under inert conditions bears the risk of oxygen migration and re-creation of a pyrophoric surface. Passivation in O_2 does provide short-term protection for rapid transfer of samples.

The situation for W_2C is different; regeneration of oxygen-passivated W_2C is much less effective than for Mo_2C. Catalytic activities of regenerated catalyst that had been passivated with either 0.1% or 1% O_2 are almost the same, and much less active than the in situ prepared W_2C. Even regeneration in a mixture of ethane/H_2 at the original synthesis temperature does not cause regeneration of active sites, which is problematic for correlation of results obtained with non-passivated samples to those obtained with passivated and subsequently reduced samples.

The activity of Mo_2C and W_2C surfaces that had undergone reduction with removal of oxygen or carbon could be enhanced by an additional treatment in H_2/toluene at a pressure of 20 bar and temperatures of 300 or 400 °C. When oxygen-passivated Mo_2C is reduced and then used for

toluene hydrogenation at higher temperature and 20 bar, its activity for this reaction at 150 °C is even higher than that of a fresh sample. This enhancement is most pronounced after the surface has been depleted of carbon.

Acknowledgement

Acknowledgment is made to the Donors of the American Chemical Society Petroleum Research Fund for support (or partial support) of this research under PRF#51448-ND5. This work was, in part, supported by NSF award 0923247 (thermal analysis equipment as part of a major research instrumentation grant). The authors thank Lance L. Lobban for providing the test reactor and Raul F. Lobo for access to chemisorption equipment.

References

[1] R.B. Levy, M. Boudart, Platinum-like behavior of tungsten carbide in surface catalysis, Science 181 (1973) 547-549.

[2] S.T. Oyama, Preparation and catalytic properties of transition metal carbides and nitrides, Catal. Today 15 (1992) 179-200.

[3] P. Da Costa, J.-L. Lemberton, C. Potvin, J.-M. Manoli, G. Perot, M. Breysse, G. Djega-Mariadassou, Tetralin hydrogenation catalyzed by Mo_2C/Al_2O_3 and WC/Al_2O_3 in the presence of H_2S, Catal. Today 65 (2001) 195-200.

[4] S. Ramanathan, S.T. Oyama, New catalysts for hydroprocessing: Transition metal carbides and nitrides. J. Phys. Chem. 99 (1995) 16365-16372.

[5] S. Ma, X. Guo, L. Zhao, S. Scott, X. Bao, Recent progress in methane dehydroaromatization: From laboratory curiosities to promising technology, J. Energy Chem. 22 (2013) 1-20.

[6] T. Xiao, A. Hanif, A.P.E. York, J. Sloan, M.L.H. Green, Study on preparation of high surface area tungsten carbides and phase transition during the carburisation, Phys. Chem. Chem. Phys. 4 (2002) 3522-3529.

[7] W. Zheng, T.P. Cotter, P. Kaghazchi, T. Jacob, B. Frank, K. Schlichte, W. Zhang, D.S. Su, F. Schüth, R. Schlögl, Experimental and theoretical investigation of molybdenum carbide and nitride as catalysts for ammonia decomposition, J. Am. Chem. Soc. 135 (2013) 3458-3464.

[8] J.A. Schaidle, A.C. Lausche, L.T. Thompson, Effects of sulfur on Mo_2C and Pt/Mo_2C catalysts: Water gas shift reaction, J. Catal. 272 (2010) 235-245.

[9] K. Xiong W. Yu, J.G. Chen, Selective deoxygenation of aldehydes and alcohols on molybdenum carbide (Mo_2C) surfaces, Appl. Surf. Sci. 323 (2014) 88–95.

[10] J.S. Lee, S.T. Oyama, M. Boudart, Molybdenum carbide catalysts: I. Synthesis of unsupported powders. J. Catal. 106 (1987) 125-133.

[11] A. Hanif, T. Xiao, A.P.E. York, J. Sloan, M.L. Green, Study on the structure and formation mechanism of molybdenum carbides, Chem. Mater. 14 (2002) 1009-1015.

[12] J.S. Lee, M. Boudart, Hydrodesulfurization of thiophene over unsupported molybdenum carbide. Appl. Catal. 19 (1985) 207-210.

[13] M.K. Neylon, S. Choi, H. Kwon, K.E. Curry, L.T. Thompson, Catalytic properties of early transition metal nitrides and carbides: *n*-butane hydrogenolysis, dehydrogenation and isomerization. Appl. Catal. A: Gen. 183 (1999) 253-263.

[14] J.M. Giraudon, L. Leclercq, G. Leclercq, A. Lofberg, A. Frennet, Organometallic route to dimolybdenum carbide via a low-temperature pyrolysis of a dimolybdenum alkyne complex, J. Mater. Sci. 28 (1993) 2449-2454.

[15] T. Xiao, H. Wang, A.P.E. York, V.C. Williams, M.L.H. Green, Preparation of nickel–tungsten bimetallic carbide catalysts. J. Catal. 209 (2002) 318-330.

[16] A.S. Rocha, A.B. Rocha, V.T. da Silva, Benzene adsorption on Mo_2C: A theoretical and experimental study, Appl. Catal. A: Gen. 379 (2010) 54-60.

[17] G. Leclercq, M. Kamal, J.-F. Lamonier, L. Feigenbaum, P. Malfoy, L. Leclercq, Treatment of bulk group VI transition metal carbides with hydrogen and oxygen. Appl. Catal. A: General 121 (1995) 169-190.

[18] X.Q. Zhao, Y. Liang, Z.Q. Hu, B.X. Liu, Oxidation characteristics and magnetic properties of iron carbide and iron ultrafine particles, J. Appl. Phys. 80 (1996) 5857-5860.

[19] E.M. Zahidi, H. Oudghiri-Hassani, P.H. McBreen, Formation of thermally stable alkylidene layers on a catalytically active surface, Nature 409 (2001) 1023-1026.

[20] H. Oudghiri-Hassani, E. Zahidi, M. Siaj, J. Wang, P.H. McBreen, Passivation of metal carbide surfaces: relevance to carbon nanotube–metal interconnections, Appl. Surf. Sci. 212–213 (2003) 4-9.

[21] A. Warren, A. Nylund, I. Olefjord, Oxidation of tungsten and tungsten carbide in dry and humid atmospheres, Int. J. Refract. Metals and Hard Mater. 14 (1996) 345-353.

[22] W. Wu, Z. Wu, C. Liang, P. Ying, Z. Feng, C. Li, An IR study on the surface passivation of Mo_2C/Al_2O_3 catalyst with O_2, H_2O and CO_2, Phys. Chem. Chem. Phys. 6 (2004) 5603-5608.

[23] Y. Bogatin, M. Robinson, J. Ormerod, Water milling and gas passivation method for production of corrosion resistant Nd-Fe-B-N/C powder and magnets, J. Appl. Phys. 70 (1991) 6594-6596.

[24] H. Shou, D. Ferrari, D.G. Barton, C.W. Jones, R.J. Davis, Influence of passivation on the reactivity of unpromoted and Rb-promoted Mo_2C nanoparticles for CO hydrogenation, ACS Catal. 2 (2012) 1408-1416.

[25] K.J. Leary, J.N. Michaels, A.M. Stacy, The use of TPD and TPR to study subsurface mobility: Diffusion of oxygen in Mo_2C, J. Catal. 107 (1987) 393-406.

[26] A.L. Stottlemyer, T.G, Kelly, Q. Meng, J.G. Chen, Reactions of oxygen-containing molecules on transition metal carbides: Surface science insight into potential applications in catalysis and electrocatalysis, Surf. Sci. Reports 67 (2012) 201-232.

[27] M. J. Ledoux, C.P. Huu, J. Guille, H. Dunlop, Compared activities of platinum and high specific surface area Mo_2C and WC catalysts for reforming reactions: I. Catalyst activation and stabilization: Reaction of *n*-hexane, J. Catal. 134 (1992) 383-398

[28] B. Frank, T.P. Cotter, M.E. Schuster, R. Schlögl, A. Trunschke, Carbon dynamics on the molybdenum carbide surface during catalytic propane dehydrogenation, Chem. – A European J. 19 (2013) 16938-16945.

[29] E. Iglesia, F.H. Ribeiro, M. Boudart, J.E. Baumgartner, Synthesis, characterization, and catalytic properties of clean and oxygen-modified tungsten carbides, Catal. Today 15 (1992) 307-337.

[30] E. Iglesia, J.E. Baumgartner, F.H. Ribeiro, M. Boudart, Bifunctional reactions of alkanes on tungsten carbides modified by chemisorbed oxygen, J. Catal. 131 (1991) 523-544.

[31] A.S. Mamède, J.-M. Giraudon, A. Löfberg, L. Leclercq, G. Leclercq, Hydrogenation of toluene over β-Mo_2C in the presence of thiophene, Appl. Catal. A: General 227 (2002) 73–82.

[32] G. Vitale, H. Guzmán, M.L. Frauwallner, C.E. Scott, P. Pereira-Almao, Synthesis of nanocrystalline molybdenum carbide materials and their characterization, Catal. Today 250 (2015) 123–133.

[33] G. Vitale, M.L. Frauwallner, E. Hernandez, C.E. Scott, P. Pereira-Almao, Low temperature synthesis of cubic molybdenum carbide catalysts via pressure induced crystallographic orientation of MoO_3 precursor, Appl. Catal. A: General 400 (2011) 221–229.

[34] J.W. Thybaut, M. Saeys, G.B. Marin, Hydrogenation kinetics of toluene on Pt/ZSM-22, Chem. Eng. J. 90 (2002) 117–129.

[35] J. Cai, S. Bennici, J. Shen, A. Auroux, Influence of N addition in mesoporous carbons used as supports of Pt, Pd and Ru for toluene hydrogenation and iron oxide for benzene oxidation, Reac. Kinet. Mech. Cat. 115 (2015) 263–282.

[36] S.T. Oyama, J.C. Schlatter, J.E. Metcalfe, J.M. Lambert, Jr., Preparation and characterization of early transition-metal carbides and nitrides, Ind. Eng. Chem. Res. 27 (1988) 1639-1648.

[37] M.-L. Frauwallner, F. Lόpez-Linares, J. Lara-Romero, C.E. Scott, V. Ali, E. Hernández, P. Pereira-Almao, Toluene hydrogenation at low temperature using a molybdenum carbide catalyst, Appl. Catal. A: General 394 (2011) 62–70.

[38] J.R. dos Santos Politi, F. Viñes, J.A. Rodriguez, F. Illas, Atomic and electronic structure of molybdenum carbide phases: bulk and low Miller-index surfaces, Phys. Chem. Chem. Phys. 15 (2013) 12617.

[39] X.-R. Shi, S.-G. Wang, J. Hu, Z. Qin, J. Wang, Theoretical studies on chemisorption of oxygen on β-Mo_2C catalyst and its surface oxidation, Surf. Sci. 606 (2012) 1187-1194.

[40] L.Ó. János Kiss, A.P. Farkas, F. Solymosi, Surface and subsurface oxidation of Mo_2C/Mo(100): Low-energy ion-scattering, Auger electron, angle-resolved X-ray Photoelectron, and mass spectroscopy studies, J. Phys. Chem. B 109 (2005) 4638-4645.

[41] K.J. Leary, J.N. Michaels, A.M. Stacy, Carbon and oxygen atom mobility during activation of Mo_2C catalysts, J. Catal. 101 (1986) 301-313.

[42] A.J. Medford, A. Vojvodic, F. Studt, F. Abild-Pedersen, J.K. Nørskov, Elementary steps of syngas reactions on Mo_2C(001): Adsorption thermochemistry and bond dissociation, J. Catal. 290 (2012) 108-117

[43] F. Solymosi, A. Oszkó, T. Bánsági, P. Tolmacsov, Adsorption and reaction of CO_2 on Mo_2C catalyst, J. Phys. Chemistry B 106 (2002) 9613-9618.

[44] A.R.S. Darujati, D. C. LaMont, W.J. Thomson, Oxidation stability of Mo_2C catalysts under fuel reforming conditions, Appl. Catal. A: General 253 (2003) 397-407.

[45] M.D. Porosoff, X. Yang, J.A. Boscoboinik, J.G. Chen, Molybdenum carbide as alternative catalysts to precious metals for highly selective reduction of CO_2 to CO, Angew. Chem. 126 (2014) 6823-6827.

[46] M. Nagai, K. Oshikawa, T. Kurakami, T. Miyao, S. Omi, Surface properties of carbided molybdena-alumina and its activity for CO_2 hydrogenation, J. Catal. 180 (1998) 14-23.

[47] H. Tominaga, M. Nagai, Density functional study of carbon dioxide hydrogenation on molybdenum carbide and metal, Appl. Catal. A: General 282 (2005) 5-13.

[48] N. Liu, S.A. Rykov, J.G. Chen, A comparative surface science study of carbide and oxycarbide: the effect of oxygen modification on the surface reactivity of C/W(111), Surf. Sci. 487 (2001) 107-117.

[49] T.P. St. Clair, S.T. Oyama, D.F. Cox, CO and O_2 adsorption on α-Mo_2C (0001), Surf. Sci. 468 (2000) 62-76.

[50] H.H. Hwu, M.B. Zellner, J.G. Chen, The chemical and electronic properties of oxygen-modified C/Mo(110): a model system for molybdenum oxycarbides, J. Catal. 229 (2005) 30-44.

[51] B. Vidick, J. Lemaitre, B. Delmon, Control of the catalytic activity of tungsten carbides: II. Physicochemical characterizations of tungsten carbides, J. Catal. 99 (1986) 428-438.

[52] G.S. Ranhotra, G.W. Haddix, A.T. Bell, J.A. Reimer, Catalysis over molybdenum carbides and nitrides I. Catalyst characterization, J. Catal. 108 (1987) 24-39.

[53]W.-S. Lee, Z. Wang, R.J. Wu, A. Bhan, A., Selective vapor-phase hydrodeoxygenation of anisole to benzene on molybdenum carbide catalysts, J. Catal. 319 (2014) 44–53.

[54] F.H. Ribeiro, R.A. Dalla Betta, M. Boudart, J. Baumgartner, E. Iglesia, Reactions of neopentane, methylcyclohexane, and 3,3-dimethylpentane on tungsten carbides: The effect of surface oxygen on reaction pathways, J. Catal. 130 (1991) 86-105.

[55] E. Iglesia, F.H. Ribeiro, M. Boudart, J.E. Baumgartner, Synthesis, characterization, and catalytic properties of clean and oxygen-modified tungsten carbides, Catal. Today 15 (1992) 307–337.

[56] V.V. Pushkarev, K. An, S. Alayoglu, S.K. Beaumont, G.A. Somorjai, Hydrogenation of benzene and toluene over size controlled Pt/SBA-15 catalysts: Elucidation of the Pt particle size effect on reaction kinetics, J. Catal. 292 (2012) 64–72.

[57] S.D. Lin, M.A. Vannice, Hydrogenation of aromatic hydrocarbons over supported Pt catalysts. 2. Toluene hydrogenation, J. Catal. 143 (1993) 554-562.

[58] P.S.F. Mendes, G. Lapisardi, C. Bouchy, M. Rivallan, J.M. Silva, M.F. Ribeiro, Hydrogenating activity of Pt/zeolite catalysts focusing acid support and metal dispersion influence, Appl. Catal. A: General 504 (2015) 17-28.

[60] J.S. Lee, K.H. Lee, J.Y. Lee, Selective chemisorption of carbon monoxide and hydrogen over supported molybdenum carbide catalysts, J. Phys. Chem. 96 (1992) 362-366.

[61] J.-S. Choi, G. Bugli, G. Djéga-Mariadassou, Influence of the degree of carburization on the density of sites and hydrogenating activity of molybdenum carbides, J. Catal. 193 (2000) 238-247.

[62] S. Eijsbouts, On the flexibility of the active phase in hydrotreating catalysts, Appl. Catal. A: General 158 (1997) 53-92.

[63] R. Prins, M. Jian, M. Flechsenhar, Mechanism and kinetics of hydrodenitrogenation, Polyhedron 16 (1997) 3235-3246.

Passivation Agents and Conditions for Mo_2C and W_2C:
Effect on Catalytic Activity for Toluene Hydrogenation

*Ali Mehdad, Rolf E. Jentoft, and Friederike C. Jentoft**

Supporting Information

A Calculations of conversions and turnover frequencies

Conversion X in % was calculated using Equation S 1:

$$X(\%) = \frac{\dot{n}_{tol,in} - \dot{n}_{tol,out}}{\dot{n}_{tol,in}} \times 100\%$$

Equation S 1

With $\dot{n}_{tol}$ the molar flow rate of toluene in or out of the reactor, respectively.

The rate of conversion of toluene r_{tol} was calculated according to Equation S 2.

$$r_{tol} = \frac{X}{100\%} \frac{F_{tol}\,\rho_{tol}}{m_{cat}\,MW_{tol}}$$

Equation S 2

With X the conversion in %, F_{tol} the volumetric liquid feed flow rate of toluene, ρ_{tol} the density of liquid toluene at room temperature (0.8669 g cm^{-3}), m_{cat} the mass of carbide, MW_{tol} the molecular weight of toluene (92.14 g mol^{-1}).

Turnover frequency was calculated using Equation S 3.

$$TOF = \frac{r_{tol}}{Sites_{CO}}$$

Equation S 3

With r_{tol} the rate of toluene conversion in moles per second and gram carbide and $Sites_{CO}$ the number of sites per gram carbide as determined by CO adsorption.

B Assessment of possible pore diffusion limitation using the Weisz-Prater criterion

Toluene conversion on fresh Mo_2C at a reaction temperature of 423 K was used as an example. All estimates are conservative, for example, the upper end of the particle size range was used. Fresh Mo_2C also has the smallest of all measured pore sizes at 2.9 nm (Table 1).

1. Identification of type of diffusion and overall diffusivity

The Knudsen number can be used to determine whether regular or Knudsen diffusion is prevailing [1]. The Knudsen number K_n is the ratio of the mean free path of the gas molecules λ and the pore diameter d_p, as shown in Equation S 4.

$$K_n = \frac{\lambda}{d_p}$$

Equation S 4

The mean free path, accounting for the Maxwell distribution, was calculated from the particle density ${}^1N$, and the hard sphere diameters cross section σ_{hs} according to Equation S 5.

$$\lambda = \frac{1}{{}^1N\,\sigma_{hs}\sqrt{2}}$$

Equation S 5

The particle density ${}^1N$ was obtained from the pressure p, the temperature T and the Boltzmann constant k according to Equation S 6.

$${}^1N = \frac{p}{kT}$$

Equation S 6

The cross section for two types of molecules was calculated from their hard sphere diameters d_1 and d_2 according to Equation S 7.

$$\sigma_{hs} = \pi\left(\frac{d_1}{2} + \frac{d_2}{2}\right)^2$$

Equation S 7

Substituting the values from Table S1, one obtains:

$K_n = 1.18$

This result means that the mean free path and the pore size are on the same order of magnitude, and both mechanisms of diffusion may occur.

In this case, an overall diffusivity D_t can be estimated from the binary diffusion coefficient D_{12} and the Knudsen diffusion coefficient D_K with the help of Equation S 8 [1].

$$\frac{1}{D_t} = \frac{1}{D_{12}} + \frac{1}{D_K}$$

Equation S 8

Table S1: Values used in Knudsen number calculations and sources

Constant or Parameter	*Value and unit*	*Source*
Boltzmann constant *k*	$1.38*10^{-23}$ J K^{-1}	
Reaction pressure *p*	21 bar	This work
Reaction temperature *T*	423 K	This work
Pore diameter d_p	2.9 nm	This work, from N_2 adsorption on Mo_2C, Table 1.
Toluene, hard sphere diameter	568 pm	[2]
H_2, hard sphere diameter	287 pm	[3]

2. Calculation of effective diffusivities

The diffusivity in a binary system can be calculated according to Equation S 9 [4, p.539].

$$D_{12} = 0.0026280 \frac{\sqrt{T^3(M_1+M_2)/2M_1M_2}}{p\sigma_{12}\Omega_{12}^{(1,1)*}(T_{12}^*)}$$

Equation S 9

With D_{12} the diffusion coefficient in cm^2/s, *p* the pressure in atmospheres, *T* the temperature in Kelvin, M_1 and M_2 the molecular weights of species 1 and 2, σ_{12} a molecular potential energy parameter characteristic of 1-2 interaction in Å as defined in Equation S 10, T_{12}^* as defined in Equation S 12, and Ω an integral dependent on temperature and the molecular potential energy parameters.

The molecular potential energy parameters σ_{12} and ϵ_{12} characteristic of 1-2 (toluene-H_2) interaction are obtained using Equation S 10 and Equation S 11.

$$\sigma_{12} = 0.5(\sigma_1 + \sigma_2)$$

Equation S 10

$$\epsilon_{12} = \sqrt{\epsilon_1\epsilon_2}$$

Equation S 11

T_{12}^* is calculated using Equation S 12 [4].

$$T_{12}^* = \frac{kT}{\epsilon_{12}}$$

Equation S 12

Using the values in Table S2, the following results were obtained:

σ_{12} = 4.28 Å

ϵ_{12}/k = 148 K

T_{12}^*= 2.86

Ω was found by interpolation between the values reported for T^*=2.8 and T^*=2.9 [4, p. 1127].

Ω = 0.961.

Substituting these values into Equation S 9, the binary diffusion coefficient is obtained:

D_{12} = 4.72 ×10^{-2} cm^2 s^{-1}

The Knudsen diffusion coefficient D_K is given by Equation S 13 [1].

$$D_K = \frac{d_p}{3}\sqrt{\frac{8\,R\,T}{\pi\,MW}}$$

Equation S 13

With d_p the pore diameter in m, R the ideal gas constant (8.314 J mol^{-1} K^{-1}) and MW the molecular weight (using toluene as the reactant with the smaller diffusivity).

The results for D_K and the overall diffusivity D_t (Equation S 8) were

D_K = 3.01×10^{-3} cm^2 s^{-1}

D_t = 2.83×10^{-3} cm^2 s^{-1}

The effective overall diffusivity $D_{t,eff}$ was calculated using Equation S 14 [5].

$$D_{t,eff} = \frac{D_t\,\varphi\,\sigma_{cons}}{\tau}$$

Equation S 14

With φ the porosity, σ_{cons} the constriction factor, and τ the tortuosity.

Using values for these parameters listed in Table S2:

$D_{t,eff}$ = 3.02 × 10^{-4} cm^2 s^{-1}

Table S2: Values used in diffusivity calculations and sources

Constant or Parameter	*Value and unit*	*Source*
Reaction temperature T	423 K	This work
Reaction pressure p	20.73 atm	This work
Toluene, molecular potential energy interaction parameter σ	5.64 Å	[3]
Toluene, molecular potential energy interaction parameter ϵ/k	575 K	[3]
Toluene, molecular weight	92.14 g mol^{-1}	
H_2, molecular potential energy interaction parameter σ	2.915 Å	[4, p. 1110]
H_2, molecular potential energy interaction parameter ϵ/k	38 K	[4, p. 1110]
H_2, molecular weight	2.02 g mol^{-1}	
Porosity φ	0.4	[5]
Tortuosity τ	3	[5]
Constriction factor σ_{cons}	0.8	[5]

3. Calculation of the Weisz-Prater criterion

The criterion formulated by Weisz and Prater [6] for measured reaction rates is given in Equation S 15.

$$\frac{R^2}{D_{eff}} \frac{1}{c} \frac{dn_V}{dt} \leq 1$$

Equation S 15

With R the particle radius, c the reactant concentration in moles per volume and dn_V/dt the reaction rate per volume of catalyst.

The following values were used

R = 5 µm (as the upper end of the secondary particle size range of 1-10 µm typical of Mo_2C produced from commercial MoO_3 via carburization [7])

$c = 1.6 \times 10^{-5}$ mol cm^{-3} (considering toluene, the reactant with the smaller concentration)

r_{tol} = 0.091 mol g^{-1} h^{-1} (from fresh Mo_2C, same data as in the first row of Table 3; to obtain the rate per volume, a calculated density of 9.1 g cm^{-3} for Mo_2C specified in the ICCD pdf file 00-035-0787 was used)

With these values, the left hand term of Equation S 15 is calculated to 0.003, thus allowing pore diffusion limitations to be excluded for this particular data set and also for all other data sets, because conditions and measured values do not extend over a significant range.

References

[1] W. He, W. Lv, J.H. Dickerson, Gas Transport in Solid Oxide Fuel Cells, Springer, 2014, pp 9-17.
[2] M. M. Miedaner, A. A. Migdisov, A. E. Williams-Jones, Geochimica et Cosmochimica Acta 69 (2005) 5511–5516.
[3] E. Wilhelm, R. Battino, J. Chem. Phys. 55 (1971) 4012-4017.
[4] J.O. Hirschfelder, C.F. Curtiss, R.B. Bird, Molecular Theory of Gases and Liquids, John Wiley & Sons, Inc. New York, Fourth Printing 1967.
[5] H. Scott Fogler, Elements of Chemical Reaction Engineering, Fifth Edition, Prentice Hall, Boston, 2016 (Ebook edition).
[6] P.B. Weisz, C.D. Prater, Adv. Catal. 6 (1954) 143-196.
[7] G. Vitale, M.L. Frauwallner, E. Hernandez, C.E. Scott, P. Pereira-Almao, Appl. Catal. A: General 400 (2011) 221-229.